Cycloaddition Behaviour of Pyrazol-4-one *N,N*-Dioxides toward Unsaturated Compounds. Stereochemical and Mechanistic Aspect

Masashi Eto, Yasuyuki Yoshitake, Kazunobu Harano and Takuzo Hisano *
Faculty of Pharmaceutical Sciences, Kumamoto University, 5-1 Oe-honmachi, 862 Kumamoto, Japan

The cycloaddition behaviour of 2,5-disubstituted pyrazol-4-one *N,N*-dioxide **1a–c** toward various unsaturated compounds **2** was investigated. The structures of the products were determined on the basis of the ^1H and ^{13}C NMR spectral data together with the X-ray crystallographic data. In general, the predominant formation of the *exo* 1,3-dipolar cycloadducts was observed. The cycloaddition behaviour of **1a–c** toward **2** is discussed on the basis of the kinetic and computational data.

Pyrazol-4-one *N,N*-dioxides **1** underwent cycloaddition to some simple olefinic compounds to give the 1,3-dipolar cycloadducts.[1,2] However, stereochemistry of the cycloadducts and their formation mechanism have not yet been clarified. The frontier MOs of **1** are closely similar to those of cyclopentadienones, suggesting that **1** would not only act as a 1,3-dipole but also as a 1,3-diene. On the basis of the stereospecific formation of the *endo–exo* cycloadducts from the reaction of epoxynaphthalene **2a** with **1**, we have considered that the cycloadducts **3** were not formed from the [1,4]-sigmatropic rearrangements[3] of the primary Diels–Alder cycloadducts but from direct cycloadditions of **1** and **2**.

In this paper, the cycloaddition behaviour of **1** toward general unsaturated compounds is discussed on the basis of kinetic and MO calculation data.

Results

Cycloaddition of 2,5-Disubstituted Pyrazol-4-one N,N-*Dioxide* (**1a**, **b**, **c**) *with Unsaturated Compounds* (**2a**).—Olefinic compounds subjected to cycloaddition are 1,4-epoxynaphthalene **2a**,[3] 2,5-norbornadiene **2b**,[3] *N*-vinylcarbazole **2c**, styrene **2d**, butyl vinyl ether **2e**, 1,5-cyclooctadiene **2f**, acrylonitrile **2g**, *N*-phenylmaleimide **2h**, *N*-ethoxycarbonylazepine **2i** and diphenylcyclopropenone **2j**.

2,5-Bis(methoxycarbonyl)pyrazol-4-one *N,N*-dioxide **1a** reacted with electron-rich olefins (**2a–e**) but did not show any cycloaddition reactivity toward unactivated **2f** and electron-deficient olefins **2g**, **h**. Unsaturated ring polyenes such as *N*-ethoxycarbonylazepine **2i** and diphenylcyclopropenone **2j** were also unreactive, presumably owing to steric interference.

2,5-Diphenylpyrazol-4-one *N,N*-dioxide **1b** showed moderate cycloaddition reactivity toward the olefins in comparison with the case of **1a**. The dioxide **1b** did not react with **2c**, **2g**, **2i** and **2j**.

2-Methyl-5-phenylpyrazol-4-one *N,N*-dioxide **1c** showed a similar trend as **1b**, in which two products were formed from a pair of reaction sites: the cycloaddition took place across the C2–N3→O and C5–N4→O positions.

The reaction conditions and products are summarized in Table 1. The cycloadduct(s) designated **3***xy* are formed from **1***x* and **2***y*.

Structure Determination of 1,3-*Dipolar Cycloadducts* (**3**).—The mass spectrum and elementary analyses agreed with the theoretical value for a 1:1 adduct. The IR spectrum of the products did not show the presence of a strained bridged carbonyl group (Table 2). In the cycloadducts from **1a**, two carbonyl absorption bands were observed at 1762 and 1738 cm^{-1}, attributable to non-conjugated and conjugated ester carbonyl groups, respectively. The strongest absorption band at 1570 cm^{-1} was assigned to the remaining >C=N→O group.

In general, the stereochemistries of the cycloadducts were determined on the basis of the structures of the cycloadducts derived from the attack at the Me–C=N→O moiety of the 2-

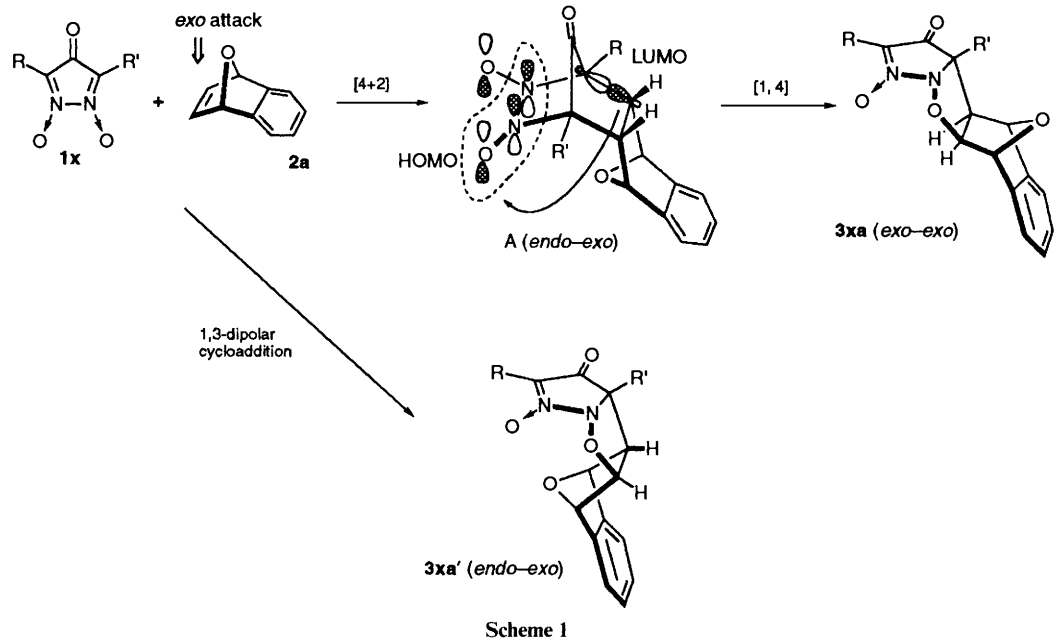

Scheme 1

Table 1 Reaction conditions and products from the reaction of **1a**, **b**, **c** with **2**

Dipole: olefin	Solvent	T/°C	Duration/h	M.p./°C	Product and yield (%)[a]	
1a:						
2a[b]	$CHCl_3$	40	4	169–170 (decomp.)	**3aa'**	70
2b[b]	$CHCl_3$	Reflux	2	168–169 (decomp.)	**3ab**	43
2c	$CHCl_3$	Reflux	2	169–170 (decomp.)	**3ac**	54
2d	$CHCl_3$	Reflux	5	153–155 (decomp.)	**3ad**	47
2e	$CHCl_3$	Reflux	8	Oil	**3ae**	50 (33)
				Oil	**3ae'**	(67)
1b:						
2a[b]	$CHCl_3$	Reflux	6	203 (decomp.)	**3ba'**	76
2b[b]	C_6H_6	Reflux	15	192–194 (decomp.)	**3bb**	38
2d	C_6H_6	Reflux	12	187–188 (decomp.)	**3bd**	63
2e	C_6H_6	Reflux	15	124–125 (decomp.)	**3be**	53 (60)[c]
					3be'	(40)[c]
2f	C_6H_6	Reflux	6	117–119 (decomp.)	**3bf**	44
2h	C_6H_6	Reflux	24	220 (decomp.)	**3bh'**	19
1c:						
2a[b]	$CHCl_3$	Reflux	5	229–230 (decomp.)	**3ca'**	46
2b[b]	$CHCl_3$	Reflux	8	139–141 (decomp.)	**3cb**	49 (28)
				133–135 (decomp.)	**3cb'**	(25)
				183–184 (decomp.)	**3'cb**	(47)
2d	$CHCl_3$	Reflux	7	178–180 (decomp.)	**3cd**	51 (65)
				107–109 (decomp.)	**3'cd**	(35)
2e	$CHCl_3$	Reflux	5	Oil	**3ce**	61 (23)
				Oil	**3ce'**	(77)
2f	$CHCl_3$	Reflux	24	142–143 (decomp.)	**3cf**	78 (43)
				Oil	**3cf'**	(20)
				157–158 (decomp.)	**3'cf**	(37)
2g	$CHCl_3$	Reflux	4	147–148 (decomp.)	**3cg'**	89 (34)
				161–163 (decomp.)	**3cg**	(66)
2h	$CHCl_3$	Reflux	8	198 (decomp.)	**3ch'**	70[d]

[a] Reaction product ratio in parenthesis. [b] Previous reported data.[3] [c] Based on the ^1H NMR spectrum. [d] The crude product included a small amount of the *exo* cycloadduct.

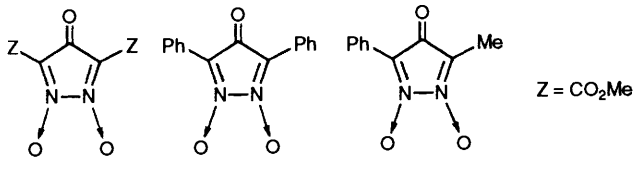

1a **1b** **1c**

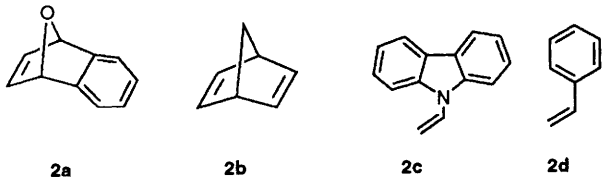

2a **2b** **2c** **2d**

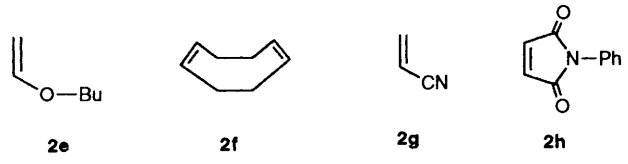

2e **2f** **2g** **2h**

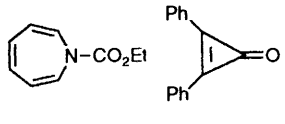

2i **2j**

methyl-5-phenyl dioxide **1c** and the X-ray crystal structure of the cycloadduct **3bd** from the 2,5-diphenyl dioxide **1b** and styrene **2d**.

In the reaction of **1c** with **2d**, **2d** reacted faster with **1c** at the Me–C=N→O moiety than at the Ph–C=N→O moiety, wherein the two cycloadducts (**3cd** and **3'cd**) were produced in 33 and 18% yields, respectively. The *exo* nature of the cycloadduct (**3cd**) was established on the NOE difference spectra obtained by irradiation of the C_2–Me group, in which significant NOE was observed between C_2–Me and the *exo* proton (Ha) which coupled with the geminal proton (Hb, J 13.2 Hz) and with the *trans* proton (Hx, J 11.4 Hz). The coupling constant between Hb and Hx is 5.86 Hz. The spectral feature was closely similar to that of the *exo* cycloadduct (**3bd**) whose structure was firmly established by single crystal X-ray analysis. These facts indicate that **3cd** is an *exo* cycloadduct, ruling out the possibility of an *endo* cycloadduct and the regioisomer. The stereochemistry of **3'cd** was determined to be *exo* on the basis of the ^1H NMR spectral pattern which resembles those of **3cd** and **3bd**.

The cycloaddition of acrylonitrile **2g** to **1c** gave a mixture of the *exo* and *endo* cycloadducts (**3cg** and **3cg'**) which derived from the attack at the methyl nitrone moiety of **1c**. In **3cg**, the NOE effect was observed between the methyl group and Ha of the methylene group, which coupled with the methine proton (Hx) on the carbon bearing the cyano group (J_{ax} 10.3 Hz). The values of J_{bx} and J_{ab} are 6.96 and 13.2 Hz, respectively. These suggest that **3cg** is an *exo* cycloadduct. Similar consideration suggests that **3cg'** is an *endo* cycloadduct, in which Hx coupled with Ha (J_{ax} 9.2 Hz) and Hb (J_{bx} 1.2 Hz).

The reaction of butyl vinyl ether **2e** with **1c** also gave a mixture of the *exo* and *endo* adducts (**3ce** and **3ce'**) formed from

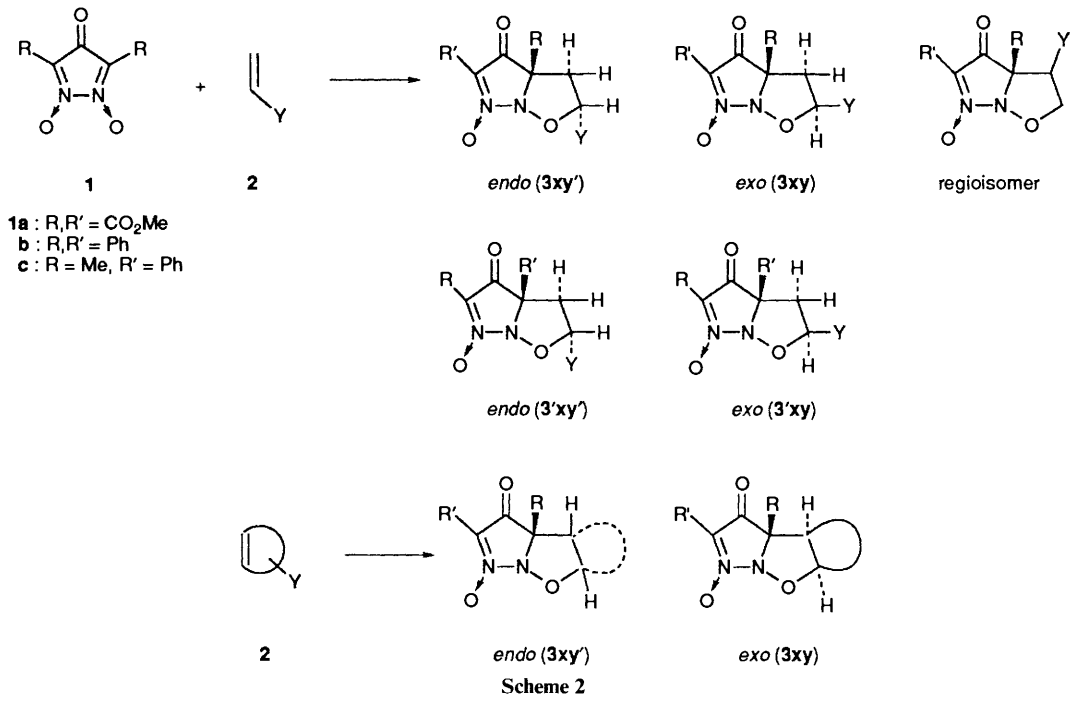

Scheme 2

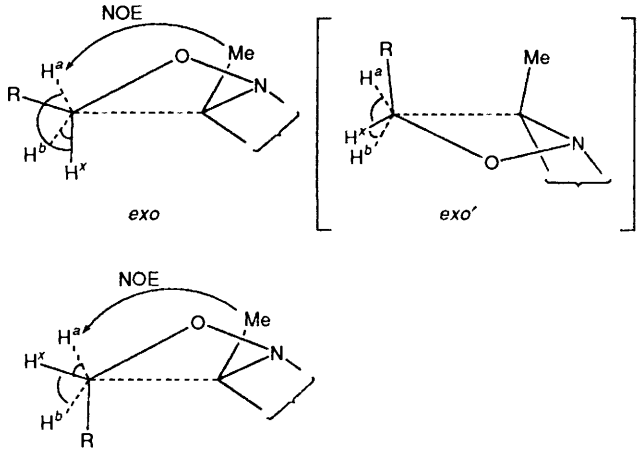

Fig. 1 Conformation of the isoxazole ring of cycloadducts 3 and dihedral angles

the attack at the methyl nitrone moiety of **1c**. In the *endo* cycloadduct (**3ce'**), the coupling constant (J_{bx}) between the *trans*-oriented protons is nearly zero, slightly smaller than the expected value. The value of J_{ax} for the *exo* cycloadduct **3ce** was observed to be 2.9 Hz, considerably smaller than expected from the Karplus equation. The magnitude of vicinal coupling constants in saturated systems is influenced by electronnegativity of substituents.[4] Taking into consideration that the electronnegativity of the carbon (–O–CH–O–) is remarkably increased by the geminal oxygens, the decrease of the J_{ax} value is considered to be very large. These facts imply that the conformation of the isoxazole ring of the *exo* cycloadduct **3ce** may be different from the one of the *endo* cycloadduct **3ce'** (see *exo'* conformation in Fig. 1).

Disubstituted olefins also readily reacted with **1a–c**. In the reaction of **1c** with 1,5-cyclooctadiene **2f**, two *exo* cycloadducts **3cf** and **3'cf** resulted from site selection. In **3'cf**, the methylene protons adjacent to the ring juncture resonate at high-field regions (1.10–1.16 and 1.35–1.44 ppm) owing to the ring current effect of the *cis*-oriented phenyl group, in agreement with *exo* cycloadduct. The structure of **3cf** was determined by comparison of the ^{1}H NMR spectral data with that of **3'cf**. *N*-Phenylmaleimide **2h** added to **1c** gave the *endo* cycloadduct **3ch**, whose structure was determined by analysis of the NOE data. Inspection of the crude product indicated the presence of a small amount of the *exo* isomer.

Detail of the structure determinations for the cycloadducts from epoxynaphthalene **2a** and norbornadiene **2b** was reported in the previous paper.[3]

Similarly, the stereo structures of the cycloadducts from **1a** and **1b** were determined on the basis of the structural data of **1c**. The ^{1}H and ^{13}C NMR spectral data are summarized in Tables 3 and 4, respectively.

Single Crystal X-Ray Analysis of the Cycloadduct (**3bd**). – To get definitive evidence for the stereochemistry of the cycloaddition, the X-ray analysis of the cycloadduct from **1b** and styrene **2d** was undertaken. The single crystals suitable for collection of the reflection data are obtained by slow evaporation of the acetone–ethanol solution. The structure was solved by direct method using MULTAN78 program[5] and refined by block-diagonal least-square method with the BDLS program.[6] The final *R* factor is 0.057. The molecular structure with numbering sequence used in this paper is depicted in Fig. 2, where each atom is represented as an ellipsoid with 30% probability. The ORTEP[7] drawing indicates that the cycloaddition proceeded through an *exo* transition state.

The dihydropyrazolone ring is planar, making an angle of 114.8° with the plane defined by C4, C5, O7 and N8. The isoxazole ring is strongly puckered, C6 being displaced 0.58 Å out-of-the-plane defined by the four atoms, C4, C5, O7 and N8. The dihedral angles between the *cis* and *trans* hydrogens of the Ph–CH–CH$_2$ moiety are 40.4 and 171.5°, respectively. The remaining nitrone moiety is interesting. Intramolecular hydrogen bondings exist between the carbonyl and nitrone oxygens and the *ortho* hydrogen atoms on the C2-phenyl ring, bringing about formation of a planar resonance structure. The angle between the dihydropyrazolone and C2-phenyl rings is 6.0°. The hydrogen-bond distances of H···O=C< and H···O←N< are 2.212 and 2.199 Å, respectively. The O←N and N–N bonds are 1.235(4) and 1.486(4) Å, respectively.

Table 2 IR Spectral and analytical data of **3**

	IR/cm^{-1}			MS		Analysis (%) Calc. (Found)		
	>C=N→O	Ester	Enone	(*m*/*z*)	Formula	C	H	N
3ac	1574	1760	1760	423 (M^+)	$C_{21}H_{17}N_3O_7$	59.58 (59.64)	4.05 (4.08)	9.92 (9.82)
3ad	1584	1754	1754	334 (M^+)	$C_{15}H_{14}N_2O_7$	53.90 (53.38)	4.22 (4.11)	8.38 (8.20)
3ae	1582	1768	1768	330 (M^+)	$C_{13}H_{18}N_2O_8$	High MS[a]		
3ae'	1582	1752	1752	330 (M^+)	$C_{13}H_{18}N_2O_8$	High MS[b]		
3bd	1560		1740	370 (M^+)	$C_{23}H_{18}N_2O_3$	74.58 (74.40)	4.90 (4.84)	7.56 (7.58)
3be + **3be'**	1556		1728	366 (M^+)	$C_{21}H_{22}N_2O_4$	68.84 (69.19)	6.05 (6.07)	7.65 (7.61)
3bf	1564		1716	374 (M^+)	$C_{23}H_{22}N_2O_3$	73.78 (73.75)	5.92 (5.90)	7.48 (7.47)
3bh'	1566		1734	439 (M^+)	$C_{25}H_{17}N_3O_5$	68.33 (68.65)	3.90 (3.91)	9.56 (9.63)
3cd	1564		1724	308 (M^+)	$C_{18}H_{16}N_2O_3$	70.12 (69.83)	5.23 (5.15)	9.09 (9.07)
3'cd	1574		1726	308 (M^+)	$C_{18}H_{16}N_2O_3$	70.12 (69.96)	5.23 (5.03)	9.09 (9.14)
3ce	1556		1724	304 (M^+)	$C_{16}H_{20}N_2O_4$	High MS[c]		
3ce'	1556		1724	304 (M^+)	$C_{16}H_{20}N_2O_4$	High MS[d]		
3cf	1560		1718	312 (M^+)	$C_{18}H_{20}N_2O_3$	69.21 (68.99)	6.45 (6.47)	8.97 (8.88)
3cf'	1566		1714	312 (M^+)	$C_{18}H_{20}N_2O_3$	High MS[e]		
3'cf	1580		1720	312 (M^+)	$C_{18}H_{20}N_2O_3$	69.21 (69.20)	6.45 (6.44)	8.97 (8.87)
3cg'	1564		1722	257 (M^+)	$C_{13}H_{11}N_3O_3$	60.70 (60.71)	4.31 (4.33)	16.33 (16.25)
3cg	1564		1722	257 (M^+)	$C_{13}H_{11}N_3O_3$	60.70 (60.65)	4.31 (4.07)	16.33 (16.14)
3ch'	1566		1730	377 (M^+)	$C_{20}H_{15}N_3O_5$	63.66 (64.13)	4.01 (4.07)	11.14 (10.86)

[a] Calc. for $C_{13}H_{18}N_2O_8$: 330.1063. Found: 330.1065. [b] Calc. for $C_{13}H_{18}N_2O_8$: 330.1063. Found: 330.1065. [c] Calc. for $C_{16}H_{20}N_2O_3$: 304.1423. Found: 304.1401. [d] Calc. for $C_{16}H_{20}N_2O_3$: 304.1423. Found: 304.1421. [e] Calc. for $C_{18}H_{20}N_2O_3$: 312.1474. Found: 312.1504.

Reaction Rates for the Cycloadditions.—To understand the general reaction behaviour of **1a–c**, the reaction rates were measured. The rates were followed by measuring the decrease of the visible absorption at 460 nm with changing temperature and solvent. The second-order rate constants for the reaction of **1a**, **b**, **c** with **2a** are listed in Table 5. From these data, the activation parameters were calculated, which are included in Table 5. The second-order rate constants for the reaction of **1a**, **b**, **c** with various olefins are listed in Table 6. The dependences of the rates on change of solvent polarity are shown in Table 7.

Molecular Orbital Calculations.—The MNDO[8] and MNDO-PM3[9] methods were used for the semiempirical MO calculations using the MOPAC[10] (version 6.02) molecular orbital package which was locally modified for a Fujitsu S-4/2 engineering workstation.

The disubstituted dioxides were approached by first combining the calculated geometry for the parent molecule (B) plus the substituents followed by a variation of all the interatomic distances plus bond and dihedral angles, until the heat of formation of the system was minimized. Similarly, the minimum energy geometries for dipolarophiles **2** were determined.

The *endo* and *exo* transition structures for the model reactions of the parent 1,3-dipole (B) with ethylene and 2-methylpyrazol-4-one *N*,*N*-dioxide (C) with acrylonitrile **2g** were determined using MNDO-PM3, which were located using the SADDLE routine[11] implemented in MOPAC and refined with the NLLSQ method[12] or TS routine[13] and characterized by establishing that the Hessian (force constant) matrix had one and only one negative eigen value.[14]

Discussion

The MNDO calculations indicate that the parent dioxide has a very low-lying LUMO energy level (−2.19 eV) in comparison with cyclopentadienone (−0.919 eV) or pyrazol-4-one (−1.83 eV) which shows extremely high cycloaddition reactivity toward various unsaturated compounds involving non-planer medium-membered ring polyenes.[15] The FMOs of **1** resemble closely those of cyclopentadienones in orbital shape, suggesting that **1** may show Diels–Alder cycloadditivity to general olefins (see Fig. 3).

In order to get some information about the cycloaddition behaviour of **1**, the structures of the transition states and products for the model 1,3-dipolar and Diels–Alder reactions were calculated. As can be seen in Fig. 4, the calculations predicted that the heat of formation of the transition structure for the Diels–Alder reaction is *ca.* 18 kcal mol^{-1}* less stable than that for the 1,3-dipolar reaction and the primary [4 + 2]π cycloadduct transforms to the cleaved product, *i.e.*, 2,5-dinitrosocyclopentanone.

The experimental results support this prediction. Dioxide **1** did not act as a diene but acted as a 1,3-dipole, showing moderate cycloaddition reactivity toward unsaturated compounds. For example, **1a** having a very low LUMO energy level

* 1 kcal mol^{-1} = 4.184 kJ mol^{-1}.

Table 3 ^{1}H NMR spectral data for the cycloadducts **3**

	^{1}H NMR δ(400 MHz); J/Hz
3ac	2.93 (1 H, dd, J 7.0, 14.3, C5-H), 4.01 (3 H, s, C12-Me), 4.01 (3 H, s, C16-Me), 4.23 (1 H, dd, J 10.3, 14.3, C5-H), 6.70 (1 H, dd, J 7.0, 9.9, C6-H), 8.05-8.07 (2 H, m, aromatic CH), 7.26-7.50 (6 H, m, aromatic CH)
3ad	2.96 (1 H, dd, J 5.9, 13.9, C5-H), 3.31 (1 H, dd, J 11.6, 13.6, C5-H), 3.90 (3 H, s, C16-Me), 3.92 (3 H, s, C12-Me), 5.02 (1 H, dd, J 5.9, 11.6, C6-H), 7.39-7.42 (5 H, m, aromatic CH)
3ae	0.86 (3 H, t, J 7.3, C20-Me), 1.15-1.28 (2 H, m, C19-H), 1.32-1.44 (2 H, m, J 6.2, 7.3, 9.2, C18-H), 2.69 (1 H, d, J 13.6, C5-H), 3.28 (1 H, dd, J 4.8, 13.6, C5-H), 3.41 (1 H, ddd, J 6.2, 7.0, 9.2, C18-H), 3.65 (1 H, ddd, J 6.2, 7.0, 9.2, C17-H), 3.85 (3 H, s, C15-Me), 3.93 (3 H, s, C11-Me), 5.51 (1 H, d, J 4.8, C6-H)
3ae'	0.91 (3 H, t, J 7.3, C20-Me), 1.29-1.38 (2 H, m, C19-H), 1.54-1.59 (2 H, m, C18-H), 2.54 (1 H, dd, J 5.1, 13.5, C5-H), 3.21 (1 H, dd, J 4.0, 13.5), 3.56 (1 H, ddd, J 6.2, 6.6, 9.5, C18-H), 3.84 (1 H, ddd, J 6.2, 6.6, 9.5, C17-H), 3.87 (3 H, s, C15-Me), 3.92 (3 H, s, C11-H), 5.49 (1 H, dd, J 4.0, 5.1, C6-H)
3bd	2.76 (1 H, dd, J 11.3, 12.8, C5-H), 3.42 (1 H, dd, J 5.5, 12.8, C5-H), 5.16 (1 H, dd, J 5.5, 11.3, C6-H), 7.23-7.49 (2 H, m, aromatic CH), 7.67-7.70 (2 H, m, aromatic CH), 8.48-8.52 (11 H, m, aromatic CH)
3be	0.68 (3 H, t, J 7.3, C13-Me), 1.07-1.29 (2 H, m, C12-H), 1.29-1.33 (2 H, m, C11-H), 2.78-2.84 (1 H, m, C5-H), 3.19 (1 H, d, J 10.8, C5-H), 3.41-3.49 (1 H, m, C10-H), 3.77-3.85 (1 H, m, C10-H), 5.52 (1 H, d, J 4.8, C6-H), 7.34-7.47 (2 H, m, aromatic CH), 7.62-7.67 (2 H, m, aromatic CH), 8.38-8.44 (6 H, m, aromatic CH)
3be'	0.83 (3 H, t, J 7.3, C13-Me), 1.18-1.26 (2 H, m, C12-H), 1.44-1.63 (2 H, m, C11-H), 2.78-2.84 (1 H, m, C5-H), 2.99 (1 H, dd, J 5.1, 13.2, C5-H), 3.49-3.53 (1 H, m, C10-H), 3.77-3.85 (1 H, m, C10-H), 5.57 (1 H, dd, J 5.0, 11.0, C6-H), 7.34-7.47 (2 H, m, aromatic CH), 7.62-7.67 (2 H, m, aromatic CH), 8.38-8.44 (6 H, m, aromatic CH)
3bf	1.11-1.13 (1 H, m, C6, 7, 10 or 11-H), 1.25-1.30 (1 H, m, C6, 7, 10 or 11-H), 1.88-1.94 (2 H, m, C6, 7, 10 or 11-H), 2.10-2.14 (2 H, m, C6, 7, 10 or 11-H), 2.35-2.43 (2 H, m, C6, 7, 10 or 11-H), 3.19-3.33 (1 H, m, J 11.3, C5-H), 4.43-4.46 (1 H, m, J 11.3, C12-H), 5.48-5.50 (1 H, m, C8-H), 5.58-5.59 (1 H, m, C9-H), 7.37-7.69 (8 H, m, aromatic CH), 8.26-8.28 (2 H, m, aromatic CH)
3bh'	4.64 (1 H, d, J 7.7, C5-H), 5.89 (1 H, d, J 7.7, C9-H), 6.75-7.25 (2 H, m, aromatic CH), 7.25-7.33 (4 H, m, aromatic CH), 7.52-7.60 (5 H, m, aromatic CH), 7.71-7.74 (2 H, m, aromatic CH), 8.10-8.13 (2 H, m, aromatic CH)
3cd	1.78 (3 H, s, C9-Me), 2.33 (1 H, dd, J 11.4, 13.2, C5-H), 2.98 (1 H, dd, J 5.9, 13.2, C5-H), 5.00 (1 H, dd, J 5.9, 11.4, C6-H), 7.25-7.53 (8 H, m, aromatic CH), 8.50-8.52 (2 H, m, aromatic CH)
3'cd	2.12 (3 H, s, C9-Me), 2.69 (1 H, dd, J 12.7, 13.2, C5-H), 3.32 (1 H, dd, J 5.4, 13.2, C5-H), 5.09 (1 H, dd, J 5.4, 11.7, C6-H), 7.33-7.43 (8 H, m, aromatic CH), 7.63-7.66 (2 H, m, aromatic CH)
3ce	0.67 (3 H, t, J 7.3, C13-Me), 1.05-1.12 (2 H, m, C12-H), 1.25-1.32 (2 H, m, C11-H), 1.65 (3 H, s, C14-Me), 2.40 (1 H, dd, J 5.1, 13.4, C5-H), 2.72 (1 H, d, J 13.4, C5-H), 3.34-3.40 (1 H, m, C10-H), 3.72-3.77 (1 H, m, C10-H), 5.44 (1 H, d, J 5.1, C6-H), 7.44-7.50 (3 H, m, aromatic CH), 8.39-8.41 (2 H, m, aromatic CH)
3ce'	0.93 (3 H, t, J 7.3, C13-Me), 1.36-1.44 (2 H, m, C12-H), 1.52-1.64 (2 H, m, C11-H), 1.75 (3 H, s, C14-Me), 2.32 (1 H, dd, J 2.9, 13.2, C5-H), 2.52 (1 H, dd, J 5.9, 13.2, C5-H), 3.52-3.61 (1 H, m, C10-H), 3.89-3.94 (1 H, m, C10-H), 5.51 (1 H, dd, J 5.9, 2.9, C6-H), 7.46-7.50 (3 H, m, aromatic CH), 8.40-8.43 (2 H, m, aromatic CH)
3cf	1.51 (3 H, s, C15-Me), 1.61-2.88 (8 H, m, C6, 7, 10 and 11-H), 2.83-2.88 (1 H, m, C5-H), 4.01-4.06 (1 H, m, C12-H), 5.51-5.62 (2 H, m, C7, 8-H), 7.45-7.52 (3 H, m, aromatic CH), 8.47-8.49 (2 H, m, aromatic CH)
3'cf	1.62 (3 H, s, C15-Me), 1.49-2.56 (8 H, m, C6, 7, 10 and 11-H), 2.62-2.68 (1 H, m, C5-H), 4.85-4.91 (1 H, m, C12-H), 5.47-5.62 (2 H, m, C7, 8-H), 7.35-7.60 (3 H, m, aromatic CH), 8.41-8.49 (2 H, m, aromatic CH)
3'cf	1.13 (1 H, ddd, J 5.5, 9.5, 13.6, C6-H), 1.39 (1 H, J 5.4, 9.5, 13.6, C6-H), 1.82-2.59 (6 H, m, C7, 10 or 11-H), 2.03 (3 H, s, C15-Me), 3.17-3.22 (1 H, m, C5-H), 4.08-4.12 (1 H, m, C12-H), 5.44-5.51 (1 H, m, C9-H), 5.57-5.61 (1 H, m, C8-H), 7.26-7.41 (3 H, m, aromatic CH), 7.67-7.73 (2 H, m, aromatic CH)
3cg'	1.71 (3 H, s, C9-Me), 2.74 (1 H, dd, J 9.2, 13.9, C5-H), 3.06 (1 H, dd, J 1.2, 13.9, C5-H), 5.19 (1 H, dd, J 1.2, 9.2, C6-H), 7.50-7.52 (3 H, m, aromatic CH), 8.37-8.39 (2 H, m, aromatic CH)
3cg	1.74 (3 H, s, C9-Me), 2.62 (1 H, dd, J 10.3, 13.2, C5-H), 3.10 (1 H, dd, J 7.0, 13.2, C5-H), 4.67 (1 H, dd, J 7.0, 10.3, C6-H), 7.47-7.51 (3 H, m, aromatic CH), 8.39-8.41 (2 H, m, aromatic CH)
3ch'	1.76 (3 H, s, C12-Me), 4.20 (1 H, d, J 7.7, C5-H), 5.79 (1 H, d, J 7.7, C9-H), 7.21-7.65 (8 H, m, aromatic CH), 8.10-8.35 (2 H, m, aromatic CH)

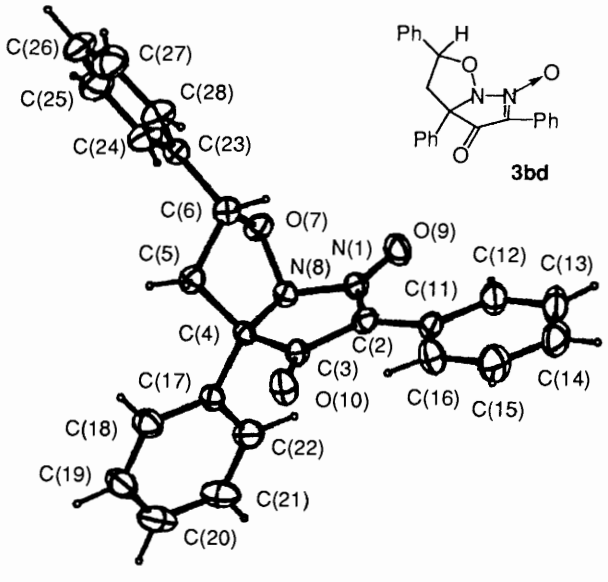

3bd

Fig. 2 ORTEP drawing to indicate the numbering sequence for the non-hydrogen atoms of **3bd**

(−2.8 eV) did not show the reactivity toward *N*-ethoxycarbonylazepine, which reacts readily with dissociating cyclopentadienones.

In the 1,3-dipolar reactions, coulombic interaction between electron-rich nitrone oxygen and olefinic carbon also plays an important role for determination of reactivity and regiochemistry. The relatively low cycloaddition reactivity of **1** and inertness of the remaining nitrone moiety of the 1:1 cycloadducts toward olefins are due presumably to the reduced LUMO coefficients and low-electron density of the oxygen atom of the nitrone. The MNDO-calculated LUMO coefficients and net charges (NC) of the reaction sites of dimethyl nitrone (D), pyrazol-4-one *N*,*N*-dioxide (E) and the 1:1 cycloadduct (F) are listed in Table 8 (see also Fig. 5). The magnitudes of the coefficients and net charges of E and F are significantly smaller than those of D.

These indicate that the decrease of the FMO electron density and net atomic charges reduces the coulombic and FMO stabilization energies (the second and third term interactions of the perturbation equation [16]).

Inspection of the rate constants for the reaction of **1a**, **b**, **c** with various olefins indicates that **1a** shows an inverse-type reaction behaviour in Sustmann's classification for cycloaddi-

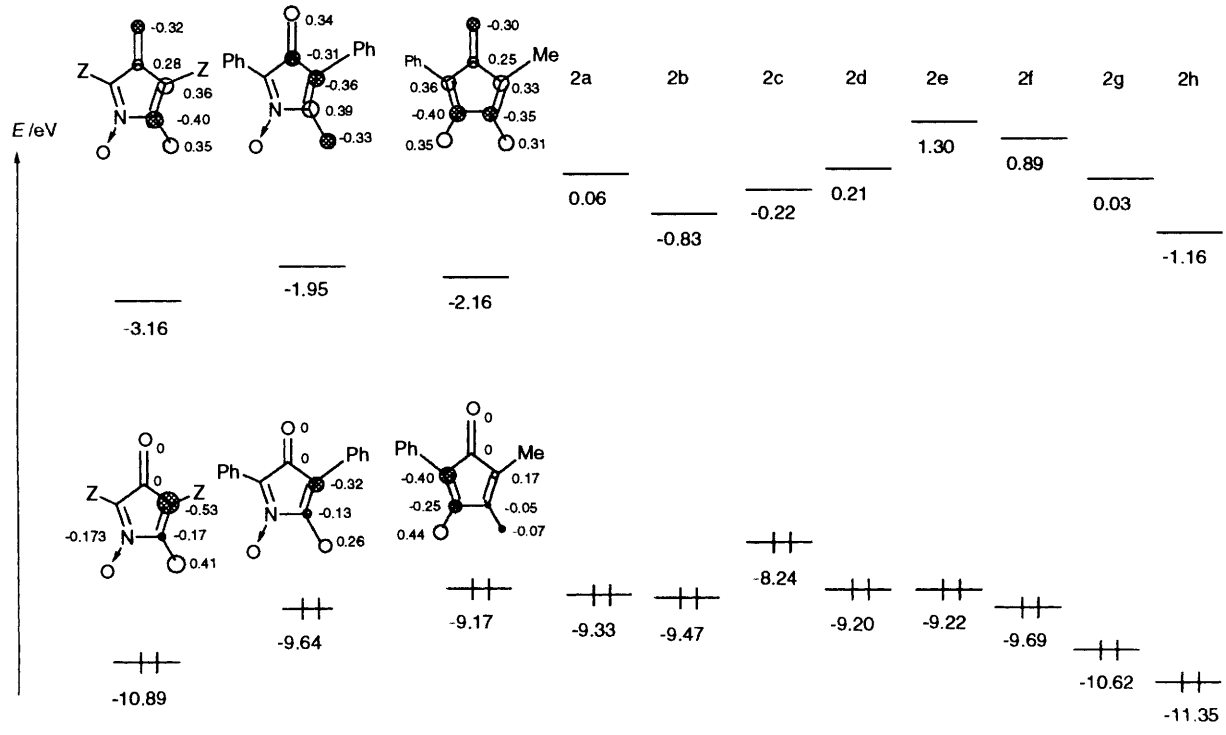

Fig. 3 FMO energy levels and coefficients of **1** and **2**

Table 4 ^{13}C NMR spectral data for the cycloadducts **3**

	^{13}C NMR (in $CDCl_3$) δ
3ac	184.1 (s), 164.9 (s), 155.9 (s), 138.8 (s), 92.4 (d), 81.5 (s), 54.7 (q), 53.0 (q), 32.7 (t)
3ad	185.8 (s), 165.0 (s), 156.2 (s), 132.9 (s), 84.8 (s), 81.6 (d), 54.5 (q), 53.2 (q), 41.4 (t)
3ae	183.2 (s), 164.1 (s), 156.3 (s), 115.1 (s), 108.5 (d), 80.3 (s), 70.6 (t), 54.2 (q), 53.1 (q), 38.3 (t), 31.3 (t), 18.9 (t), 13.7 (q)
3ae'	187.0 (s), 165.1 (s), 156.2 (s), 115.3 (s), 109.0 (d), 78.9 (s), 69.9 (t), 54.4 (q), 52.9 (q), 40.1 (t), 30.9 (t), 18.8 (t), 13.7 (q)
3bd	193.5 (s), 136.5 (s), 82.8 (d), 80.6 (s), 48.6 (t)
3be	192.2 (s), 135.5 (s), 108.3 (d), 78.6 (s), 70.3 (t), 44.3 (t), 31.4 (t), 18.9 (t), 13.6 (q)
3bf	197.1 (s), 133.2 (s), 131.0 (d), 128.6 (d), 84.0 (d), 82.6 (s), 49.3 (t), 26.3 (t), 25.7 (t), 23.7 (t), 23.6 (t)
3bh'[a]	185.4 (s), 170.6 (s), 170.5 (s), 132.7 (s), 85.0 (d), 83.2 (s), 57.3 (d)
3cd	195.6 (s), 134.6 (s), 82.9 (d), 76.3 (s), 47.4 (t), 21.6 (q)
3cd'	193.7 (s), 136.4 (s), 82.7 (d). 81.3 (s), 48.3 (t), 7.6 (q)
3ce	196.8 (s), 125.9 (s) 108.1 (d), 73.3 (s) 69.3 (t), 45.5 (t), 31.1 (t), 19.0 (t), 13.6 (q)
3ce'	194.1 (s), 124.3 (s), 108.4 (d), 74.4 (s), 70.2 (t), 42.6 (t), 31.5 (t), 19.2 (t), 13.8 (q)
3cf	198.2 (s), 130.4 (d), 128.4 (s), 127.2 (d), 84.2 (d), 77.9 (s), 47.2 (d), 26.5 (t), 25.3 (t), 23.7 (t), 22.5 (t), 17.2 (q)
3cf'	195.2 (s), 130.8 (d), 126.9 (d) 124.3 (s), 88.1 (d), 76.7 (s), 55.0 (d), 27.1 (t), 26.5 (t), 24.8 (t), 23.3 (t), 17.1 (q)
3'cf	197.0 (s), 133.1 (s), 130.1 (d), 127.1 (d), 83.9 (d), 83.5 (s), 48.8 (d), 26.0 (t), 25.7 (t), 23.7 (t), 23.6 (t), 7.5 (q)
3cg'	193.9 (s), 123.3 (s), 115.7 (s), 74.3 (s), 68.1 (d), 44.0 (t), 21.2 (q)
3cg	193.1 (s), 123.3 (s), 113.6 (s), 75.4 (s), 67.4 (d), 43.5 (t), 20.7 (q)
3ch'[a]	187.8 (s), 170.9 (s), 170.6 (s), 126.7 (s), 85.1 (d), 78.9 (s), 56.0 (d)

[a] In $[^2H_6]Me_2SO$.

Table 5 Activation parameters for the reaction of the dioxide **1a**, **b**, **c** with 1,4-epoxy-1,4-dihydronaphthalene **2a** and typical 1,3-dipolar cycloaddition reactions

Reaction T/°C	$k/10^{-6}$ s^{-1} mol^{-1} dm^3	ΔE/kcal mol^{-1}	$\Delta S^{\ddagger}$ (e.u.)
1a + **2a**			
70	19 200		
60	12 100	9.4[a]	-43
50	8 400		
40	5 000		
1b + **2a**			
70	4 565		
60	2 953	14.5[b]	-31
50	1 327		
40	620		
1c + **2a**			
70	6 393		
60	4 293	13.9[c]	-32
50	1 817		
40	973		
C,*C*-Biphenylene-*N*(α)-(*p*-chlorophenyl)-*N*(β)-cyanoazomethine imine + styrene		12.6	-31[d]
3-Bromopyridine *N*-oxide + **2a**		17.6	-31[e]

[a] Correlation coefficient, $r = 0.999$. [b] $r = 0.995$. [c] $r = 0.993$. [d] R. Huisgen, *Angew. Chem.*, 1963, **75**, 742. [e] T. Hisano, K. Harano, T. Matsuoka, T. Suzuki and Y. Murayana, *Chem. Pharm. Bull.*, 1990, **38**, 605.

tions.[17] On the other hand, **1b**, **c** shows a neutral-type reaction behaviour: a plot of the log of the rate constant for the reaction of **1b** (**1c**) against the HOMO energy level of olefins gave a rough parabola, with olefins of HOMO between 9.5 and 11 eV reacting much slower than olefins of lower or higher HOMO (see Fig. 6).

In the case of **1a**, the plot for *N*-vinylcarbazole **2c** deviates considerably from the expected point. When the reaction was followed by UV spectrometry, a slight increased absorbance in the visible region (450–600 nm) was observed. The visible absorption spectrum of the reaction mixture was not that which results from the addition of the spectra of pure samples of the two solutes, indicating the presence of a charge-transfer (CT) complex between **1a** and electron-rich dipolarophiles (Fig. 7). This suggests that the deviation is attributable to stabilization of the ground state by CT complexation.[18]

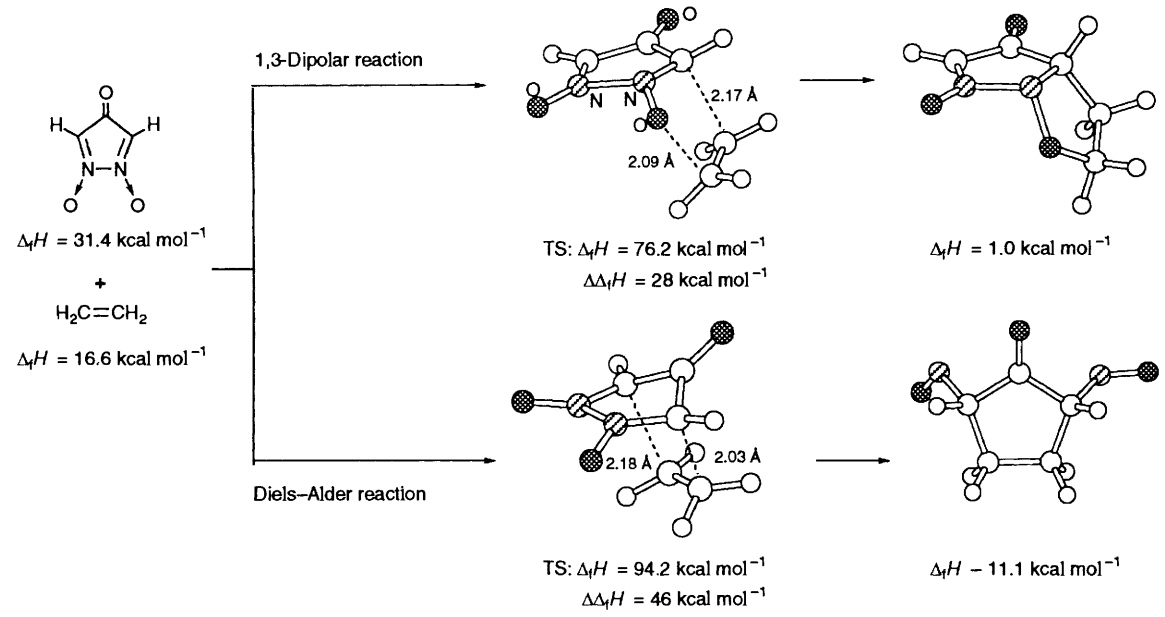

Fig. 4 PM3-calculated geometries of transition state and product for the 1,3-dipolar and Diels–Alder reactions

Table 6 Correlation between the E_i of **2** and the rates of their reaction with **1**

Dipolarophile	E_i/eV[a]	k^b/10^{-6} s^{-1} **1a**	**1b**	**1c**
N-Vinylcarbazole	8.24	672.3		
Styrene	9.20	128.9	3.55	4.76
Butyl vinyl ether	9.22	58.8	14.35	45.45
1,4-Epoxy-1,4-dihydro-naphthalene	9.33	2822	671.3	940.0
2,5-Norbornadiene	9.47	692.4	7.56	10.28
1,5-Cyclooctadiene	9.69		1.59	0.70
Acrylonitrile	10.62		0.77	1.35
N-Phenylmaleimide	11.35		4.35	7.23

[a] Negative values of the HOMO energy levels calculated by MNDO. [b] First-order rate constant at 70 °C.

Table 7 Solvent effect on rate constants k_1[a] for the reactions of **1a**, **b**, **c** with **2**

Solvent	E_T/kcal mol^{-1}	k_1/10^{-6} s^{-1} **1a** + **2d**[b]	**1b** + **2b**	**1c** + **2b**
Reaction				
Aprotic solvents				
Toluene	33.9	129.0	4.41	3.16
Dioxane	36.0	44.7	3.94	5.94
Chlorobenzene	36.8	74.3	5.52	7.97
o-Dichlorobenzene	38.0	105.6	8.15	3.99
Diethylene glycol-dimethyl ether	38.6	50.0	5.28	7.36
Dipolar aprotic solvent DMF	43.8	103.4	6.22	4.24

[a] Pseudo-first-order rate constant at 60 °C. [b] Data at 70 °C.

Inverse-type cycloaddition is energetically unfavourable because of localization of the electron density in the central part of the intermolecular region owing to the symmetric FMO coefficients (see Fig. 8). In such a case, it is suggested that the cycloaddition will presumably be less concerted or experience complex formation before giving the final product.[19] The weak response of the rate constants to variation of the polarity of the solvent rules out an intermediate involving any significant degree of charge separation.

The role of secondary orbital interactions[20] in cycloadditions

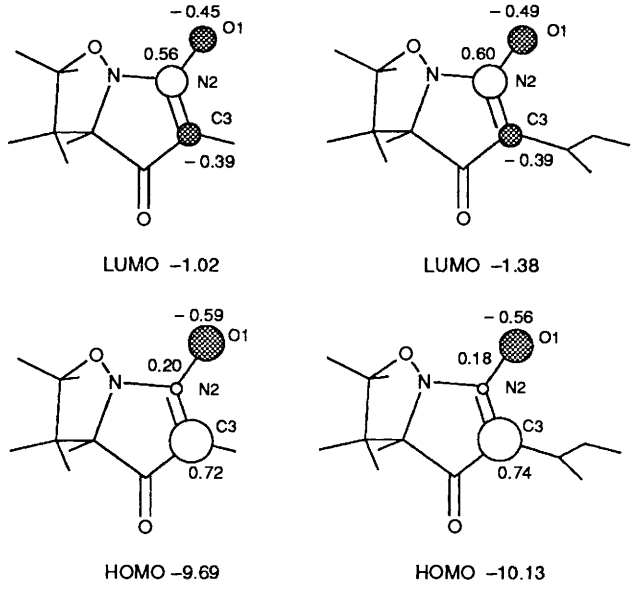

Fig. 5 FMO energy levels and coefficients of the cycloadduct (F) of C and ethylene

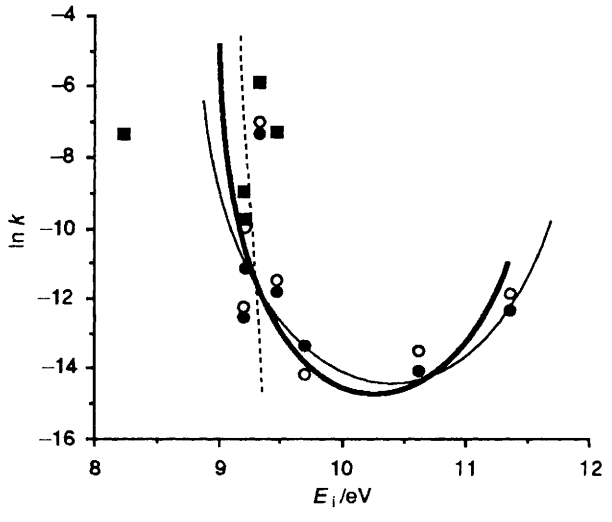

Fig. 6 Plot of the ln*k* for the reaction of **1** with **2** against the E_i values (see also Table 6): (□), **1a**; (●), **1b**; (○), **1c**

Table 8 FMO Coefficients and net charges of dimethyl nitrone (D), 2,5-dimethylpyrazol-4-one *N*,*N*-dioxide (E) and cycloadduct (F) of 2-methoxycarboylpyrazol-4-one *N*,*N*-dioxide and ethylene[a]

	HOMO/eV			LUMO/eV			NC[b]		
Atom	D	E	F	D	E	F	D	E	F
Coeff.	−8.89	−10.0	−10.1	0.15	−2.14	−1.38			
O1	−0.69	−0.41	−0.56	−0.42	−0.33	−0.49	−0.44	−0.27	−0.25
N2	0.23	0.19	0.18	0.60	0.39	0.60	0.20	0.27	0.33
C3	0.66	0.50	0.74	−0.63	−0.36	−0.39	−0.17	−0.22	−0.30

[a] Calculated by MNDO. [b] Net charge.

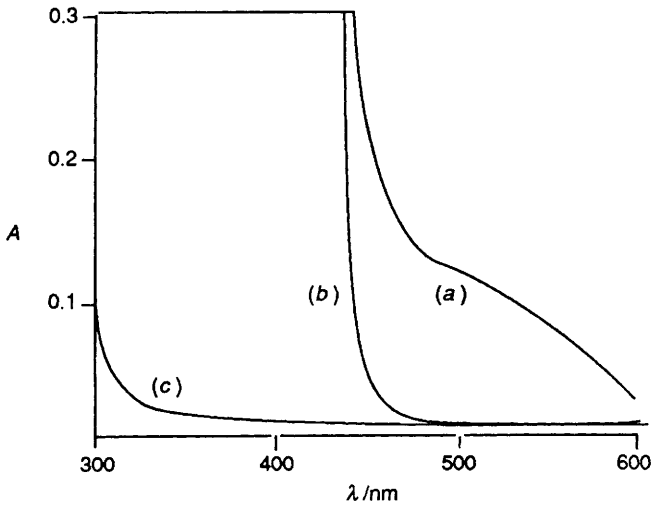

Fig. 7 Visible absorption spectrum of the mixture of **1a** and **2c**: (*a*) reaction mixture (at 0 min); (*b*) **1a**; (*c*) **2c**

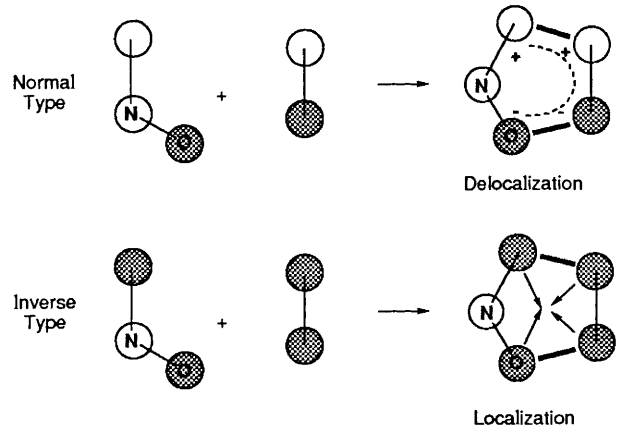

Fig. 8 FMO interactions for normal- and inverse-type 1,3-dipolar cycloadditions

has attracted much attention of organic chemists and theoreticians for prediction of the *endo*/*exo* selectivity. However, at least in nitrone cycloadditions, the predictions seem to be questionable. In this connection, we previously found that pyridine *N*-oxides cycloadd to maleimides to give only *exo* cycloadducts.[21] In the present study, *exo* cycloadducts are the main products. Based on these backgrounds, we performed MNDO-PM3 calculations on *exo* and *endo* transition structures for the reaction of the parent dioxide with acrylonitrile using SADDLE and TS routines implemented in MOPAC-V6. The PM3-calculated *exo* and *endo* transition structures are depicted in Fig. 9.

The *exo* TS structure is about 0.3 kcal mol^{-1} more stable than the *endo* one. Inspection of the *endo* structure indicates that the distance of the secondary interaction between Nβ and Cβ is 3.287 Å, in which the spatial alignment of the interacting p_z-orbitals seems to be unfavourable for effective mixing. The bond order for the secondary orbital interaction of the *endo* TS is half of that for the Diels–Alder reaction of butadiene with acrylonitrile. Gandolfi *et al.* also doubted on the role of secondary overlaps on the basis of the experimental *endo*/*exo* selectivity data for the reaction of cyclic and open-chain nitrones with *Z*-substituted dipolarophiles.[22]

The direction of addition (regioselectivity) is in agreement with predictions made on the basis of the perturbation theory: bonding always occurs between the O of the nitrone and the Cβ of the olefin R–Cβ=Cα where the largest coefficients of the interacting frontier orbitals occur. In the reactions of **1c**, two cycloadducts from site selectivity are possible. Analysis of the FMO coefficients of **1c** indicates that attack at the phenyl site is slightly better than that at the methyl site. Experimental data indicate that the main products are generally formed from attack at the methyl site, suggesting that the role of steric factors is important.

Experimental

All melting points are uncorrected. NMR spectra were taken with Hitachi R-600 (60 MHz ^{1}H NMR) and JEOL GX-400 (400 MHz ^{1}H NMR and 100 MHz ^{13}C NMR) spectrometers for 5–10% (w/v) solutions with tetramethylsilane (TMS) as an internal standard. Chemical shifts are given as δ values (ppm): s, singlet; d, doublet; dd, double doublet; t, triplet; q, quartet; br, broad; m, multiplet. IR spectra were recorded on a Hitachi 270-30 IR spectrophotometer. Mass spectra and high-resolution mass spectra were taken with a JEOL JMS-DX-300 spectrometer operating at an ionization potential of 75 eV.

MO calculations were performed on a FACOM M-780 computer and a Fujitsu S-4/2 engineering workstation.

Materials.—2,5-Bis(methoxycarbonyl)pyrazol-4-one *N*,*N*-dioxide **1a**, 2,5-diphenylpyrazol-4-one *N*,*N*-dioxide **1b** and 2-methyl-5-phenylpyrazol-4-one *N*,*N*-dioxide **1c** were prepared according to the established method.[1a] Dipolarophiles **2a–j** were commercially available materials.

Cycloaddition of 2,5-*Disubstituted-pyrazol*-4-*one* N,N-*Dioxide* **1a–c** *with Unsaturated Compounds* **2**.—*General procedure of cycloaddition.* A solution of **1** and an excess amount of an olefinic compounds in chloroform or benzene was heated at 40–80 °C until a TLC spot of **1** could not be recognized. After cooling, the solvent was evaporated off under reduced pressure. The residue was purified by chromatography on silica gel.

The results are summarized in Tables 1, 2, 3 and 4.

X-Ray Crystallographic Study.—Single crystal of **3bd** was prepared by slow evaporation of an ethanol–acetone solution. The density was measured by flotation in an aqueous potassium iodide solution, D_m = 1.337 g cm^{-3}, D_c = 1.346 g cm^{-3}. The cell

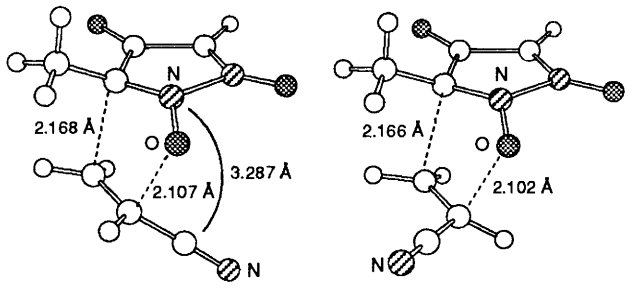

endo TS: $\Delta_f H$ = 105.14 kcal mol^{-1} *exo* TS: $\Delta_f H$ = 104.82 kcal mol^{-1}

Fig. 9 PM3-calculated transition structures from the model reaction of **1d** with **2g**

constants were obtained from least-squares refinement of the 2θ angle of 20 reflections. The crystals are monoclinic, space group $P2_1$, which was judged from the systematic absence of reflections and there are two molecules (Z = 2) in the unit cell of dimensions a = 10.467(5), b = 15.729(7), c = 5.662(2) Å, β = 101.20(3)°, V = 914(1) Å^3.

Intensity data were collected on RIGAKU AFC-6 automated diffractometer with a graphite monochromated Mo-Kα radiation (40 kV–20 mA) and by using the 2θ–ω scan mode to a limit of 2θ = 55°. Crystal stability was monitored by recording two standard reflections after every measurement of 100 reflections, and no decay was observed. A total 3593 independent reflections were measured, and after Lorentz and polarization corrections were applied, 2560 were treated as observed ($F_o > 3\ \sigma F$, $2\theta < 55°$). But no correction was applied for absorption.

The structure was solved by the direct method using the program MULTAN78.[4] An overall temperature factor was obtained from a Wilson plot. An E map calculated with signed Es ($E > 1.2$), which had the highest combined figure of merit, revealed the position of all the non-hydrogen atoms.

The structure was refined by the block-diagonal least-squares method using the program BDLS.[5] All hydrogens were placed in calculated positions. Keeping their vibrational amplitudes for the hydrogen fixed [B(H) = 3.0], and refining, we obtained a final R factor of 0.057. The weighting schemes used were w = 1.0 for $F_o < 20.0$, $w = 400/F_o^2$ for $F_o > 20.0$ for the observed reflections.

The final atomic positional parameters, anisotropic temperature factors and bond length and angles have been deposited with the Cambridge Crystallographic Data Centre.

All calculations were performed on the FACOM M-780 computer in the Kumamoto University Information Processing Center with the Universal Crystallographic Computation Program (UNICS III).[6]

Acknowledgements

The authors thank the members of the Analytical Center of this Faculty for the spectral measurements. Thanks are also due to Miss S. Nakamura for experimental assistance.

References

1 (*a*) J. P. Freeman, J. J. Gannon and D. L. Surbey, *J. Org. Chem.*, 1969, **34**, 187; (*b*) J. P. Freeman and M. L. Hoare, *J. Org. Chem.*, 1971, **36**, 19.
2 A. Kotali and P. G. Tsoungas, *Heterocycles*, 1989, **29**, 1615 and references cited therein.
3 K. Harano, Y. Yoshitake, M. Eto and T. Hisano, *Heterocycles*, 1992, **34**, 1707; M. Eto, K. Harano, Y. Yoshitake and T. Hisano, *J. Heterocycl. Chem.*, 1993, **30**, 1557.
4 L. M. Jackmann and S. Sternhell, *Applications of Nuclear Magnetic Resonance Spectroscopy in Organic Chemistry*, Pergamon Press, London, 1969, pp. 280–304.
5 P. Main, S. E. Hull, L. Lessinger, G. Germain, J. P. Declercq and M. M. Woolfson, MULTAN78, *A System of Computer Programs for the Automatic Solution of Crystal Structure from X-Ray Diffraction Data*, University of York, England, 1978.
6 T. Sakurai and K. Kobayashi, *Rikagaku Kenkyusho Hookoku*, 1979, **55**, 69; S. Kawano, *Koho, Comput. Center Kyushu Univ.*, 1983, **16**, 113.
7 C. K. Johnson, ORTEP, Report ORNL-3794, Oak Ridge National Laboratory, Oak Ridge, TN, 1965.
8 M. J. S. Dewar and W. Thiel, *J. Am. Chem. Soc.*, 1977, **99**, 4899.
9 J. J. P. Stewart, *J. Comput. Chem.*, 1989, **10**, 209; 221.
10 J. J. P. Stewart, *QCPE Bull.*, 1989, **9**, 10; revised as ver. 6.02 by the present authors for the Fujitsu S-4/2 engineering workstation.
11 M. J. S. Dewar, E. F. Healy and J. J. P. Stewart, *J. Chem. Soc., Faraday Trans. 2*, 1984, **3**, 227.
12 R. H. Bertels, Report CNA-44, 1972, University of Texas Centre for Numerical Analysis.
13 J. Bakers, *J. Comput. Chem.*, 1986, **7**, 385.
14 J. W. McIver and A. Komornicki, *J. Am. Chem. Soc.*, 1972, **94**, 2625.
15 T. Sasaki, K. Kanematsu and K. Iizuka, *J. Org. Chem.*, 1976, **41**, 1105; M. Mori, A. Hayamizu and K. Kanematsu, *J. Chem. Soc., Perkin Trans. 1*, 1981, 1259; K. Harano, M. Yasuda and K. Kanematsu, *J. Org. Chem.*, 1982, **47**, 3736; K. Harano, M. Yasuda, T. Ban and K. Kanematsu, *J. Org. Chem.*, 1980, **45**, 4455; M. Yasuda, K. Harano and K. Kanematsu, *J. Am. Chem. Soc.*, 1981, **103**, 3120.
16 G. Klopman, *J. Am. Chem. Soc.*, 1968, **90**, 223; L. Salem, *J. Am. Chem. Soc.*, 1968, **90**, 543 and 553; I. Fleming, *Frontier Orbitals and Organic Chemical Reactions*, John Wiley, London, 1976, pp. 27–32.
17 R. Sustmann, *Tetrahedron Lett.*, 1971, 2721.
18 K.-L. Mok and M. J. Nye, *J. Chem. Soc., Perkin Trans. 1*, 1975, 1810.
19 H. Fujimoto, S. Inagaki and K. Fukui, *J. Am. Chem. Soc.*, 1976, **98**, 2670; H. Fujimoto and T. Sugiyama, *J. Am. Chem. Soc.*, 1977, **99**, 15.
20 K. N. Houk, J. Sims, R. E. Duke, Jr., R. W. Strozier and J. K. George, *J. Am. Chem. Soc.*, 1973, **31**, 7287; K. N. Houk, *Pericyclic Reactions*, eds. A. P. Marchand and R. E. Lehr, Academic Press, New York, 1977, vol. 2, ch. 4 and references cited therein.
21 K. Harano, T. Matsuoka, M. Eto, T. Matsuzaki and T. Hisano, *Heterocycles*, 1989, **29**, 1029; T. Hisano, K. Harano, T. Matsuoka, H. Yamada and M. Kurihara, *Chem. Pharm. Bull.*, 1987, **35**, 1049.
22 M. Burdisso, R. Gandolfi and P. Grunanger, *J. Org. Chem.*, 1990, **55**, 3428.

Paper 3/07191J
Received 6*th December* 1993
Accepted 25*th February* 1994